Drug Design, Development and Therapy

Dovepress
open access to scientific and medical research

Open Access Full Text Article

ORIGINAL RESEARCH

Integrating Network Pharmacology and Experimental Validation to Investigate the Mechanism of Qushi Huatan Decoction Against Coronary Heart Disease

Chunxia Yin[1,*], Taohua Lan[2,3,*], Yunshan Wu[4,5], Jing Cai[1], Haoxiang Li[1], Xiaolan Kuang[1], Lin Jiao[1], Xiaomin Ou[1], Hua Yang[2], Bo Liu[3–5], Weihui Lu[2,6,7]

[1]The Second Clinical Medical College, Guangzhou University of Chinese Medicine, Guangzhou, People's Republic of China; [2]Department of Cardiology, Guangdong Provincial Hospital of Chinese Medicine, Guangzhou, People's Republic of China; [3]State Key Laboratory of Dampness Syndrome of Chinese Medicine, The Second Affiliated Hospital of Guangzhou University of Chinese Medicine, Guangzhou, People's Republic of China; [4]Guangzhou Key Laboratory of Chirality Research on Active Components of Traditional Chinese Medicine, Guangdong Provincial Hospital of Chinese Medicine, Guangzhou, People's Republic of China; [5]Guangdong Provincial Key Laboratory of Clinical Research on Traditional Chinese Medicine Syndrome, Guangzhou University of Chinese Medicine, Guangzhou, People's Republic of China; [6]State Key Laboratory of Traditional Chinese Medicine Syndrome, Guangdong Provincial Hospital of Chinese Medicine, Guangzhou University of Chinese Medicine, Guangzhou, People's Republic of China; [7]Chinese Medicine Guangdong Laboratory, Guangdong Hengqin, People's Republic of China

*These authors contributed equally to this work

Correspondence: Weihui Lu, Bo Liu, The Second Clinical Medical College, Guangzhou University of Chinese Medicine, Email weihui.lu@gzucm.edu.cn; doctliu@gzucm.edu.cn

Purpose: This study was designed to evaluate the effect and mechanism of the Qushi Huatan (QSHT) decoction against coronary heart disease (CHD) through network pharmacology and experimental verification.

Methods: In the present study, the active ingredients of the QSHT decoction were identified by ultra performance liquid chromatography/tandem mass spectrometry (UPLC/MS), then the potential ingredients and coronary heart disease targets were predicted using the SwissTarget Prediction database and the database of Genecards and OMIM database, respectively. A herb-compound-target network was constructed using Cytoscape. GO and KEGG enrichment analysis were performed using the ClusterProfiler data package of R software. Molecular docking was used to predict the core targets of QSHT against CHD. In addition, we used a myocardial infarction (MI) and high-fat diet ApoE$^{-/-}$ mice model to investigate the cardioprotective effects of QSHT. Western blotting and immunochemistry were used to verify the core targets and the signaling pathway.

Results: A total of 68 active ingredients were found in the QSHT decoction. Network pharmacology indicated 28 targets and 147 signal pathways, including AKT1, HIF-1α, GSK-3β, TLR4 and NF-κB, those key targets were also verified by molecular docking. The results of GO and KEGG enrichment analysis showed that the targets of QSHT against CHD were largely associated with inflammatory and oxidative stress, and AKT/HIF-1α and TLR4/NF-κB pathways might be key functional pathways. In vivo, QSHT significantly improved cardiac function and attenuated fibrosis and inflammation. Furthermore, QSHT could significantly inhibit the expression of HIF-1α, TLR4, phosphorylation of AKT1, GSK-3β and NF-κB after MI in ApoE$^{-/-}$ mice.

Conclusion: Based on network pharmacology, molecular docking and experimental verification, this study demonstrated that QSHT could improve cardiac function and attenuate cardiac fibrosis by regulating TLR4/NF-κB and AKT/HIF-1α signaling pathway in post-MI and high-fat diet ApoE$^{-/-}$ mice.

Keywords: network pharmacology, molecular docking, Qushi Huatan decoction, coronary heart disease

Received: 5 April 2024
Accepted: 17 August 2024
Published: 11 September 2024

Introduction

Coronary heart disease (CHD) is characterized by an inadequate supply of oxygen-rich blood to the myocardium due to arterial plaques that narrow the coronary arteries, with manifested episodic or persistent angina.[1] Epidemiological research showed that CHD is one of the leading causes of death worldwide, and its incidence population tends to be younger, which threatens human life and health.[2] In recent decades, the effects of western medicines have encountered a bottleneck, clinical practice has found that the effect of simple western medicine is not ideal, and long-term medication also increases the risk of adverse drug reactions and drug resistance.[3,4] Therefore, it is necessary to seek alternative medicines to treat CHD.

Traditional Chinese medicine (TCM), as a type of alternative drug, has shown the merits of safety and effectiveness. TCM has been shown to have a significant clinical effect in the treatment of CHD.[5] On the basis of the theory of TCM, CHD belongs to the category of "chest obstruction or heart pain". The pathogenesis of CHD is closely related to phlegm-dampness, which blocks meridians and resulting in heart pain.[6] Therefore, clinical medication should focus on removing phlegm-dampness and relieving pain. Qushi Huatan (QSHT) decoction was developed on the basis of Pingwei San by Keji Chen, who is the famous TCM expert and academician of Chinese Academy of Sciences. In composition, the QSHT decoction consists of six Chinese herbal medicines, including three herbs from Pingwei San (rhizoma atractylodis, Magnolia officinalis and dried orange peel), and the other three herbs are Rhizoma Curcumae, Acorus gramineus and Rhizoma Pinellinae Praeparata. More recently, QSHT decoction was applied in clinical to treat CHD and is effective. However, the active compounds, potential targets, and signaling pathways involved in anti-CHD have not been elucidated.

With the development of bioinformatics and system biology, network pharmacology provides us with useful tools to screen potential active ingredients and elucidate therapeutic mechanisms by constructing disease-gene-target-drug networks.[7,8] In recent years, the network pharmacology-based method has been used to manifest the "multi-compound, multi-target" characteristics of TCM. However, there exist limitations in the traditional Chinese medicine-related database, including incompleteness of data, lacking detailed descriptions about the compounds, genes, and diseases.[9] The comprehensive and complete information of ingredients of TCM is critical for accurate assessments of network pharmacology, therefore, we achieve active ingredients of QSHT decoction by ultra performance liquid chromatography/mass spectrum (UPLC/MS) analysis but not database.

In the current study, a comprehensive method is developed that combines UPLC/MS analysis with network pharmacology and experimental validation. The flow chart is illustrated in Figure 1. Briefly, (1) UPLC/MS technology was used to determine the main active components of QSHT decoction; (2) Bioinformatic analysis is used to establish the "herbs-active components-targets and pathways" network for screening potential major targets of QSHT decoction in the treatment of CHD; (3) The therapeutic effects of QSHT decoction and some key targets were experimentally validated in post-MI and high-fat diet ApoE$^{-/-}$ mice.

Materials

Chemicals and Materials

Atractylodin (Lot. 5098), Magnolol (Lot. 5672), Honokiol (Lot. 9355), Hesperidin (Lot. 7340), Nobiletin (Lot. 8005), Curdione (Lot. 9697), Curcumol (Lot. 3834), Germacrone (Lot. 7447), α-asarone (Lot. 8009), β-Asarone (Lot. 4391), Ammonium Glycyrrhizinate (Lot. 7435) were purchased from Shanghai Standard Technology Co., Ltd. (Shanghai, China). Methanol and acetonitrile (HPLC grade) were purchased from Merck Co., Ltd. The water was prepared using the RODI-200B1 water purification system (RSJ Scientific Instruments Co., ltd, Xiamen, China).

Magnolia officinalis (Lot. 220201) and Rhizoma Curcumae (Lot. 220301) were purchased from yulin materia medica Chinese herbal medicine Co., Ltd. Dried orange peel (Lot. 220401681) and rhizoma pinelliae (Lot. 22010404) were purchased from Kangmei Pharmaceutical Co., LTD, rhizoma atractylodis (Lot. 2112003) were purchased from Lingnan Chinese medicine yinpian co., LTD, Acorus gramineus (Lot. C12201094) were purchased from China Pharmaceutical Group co., LTD.

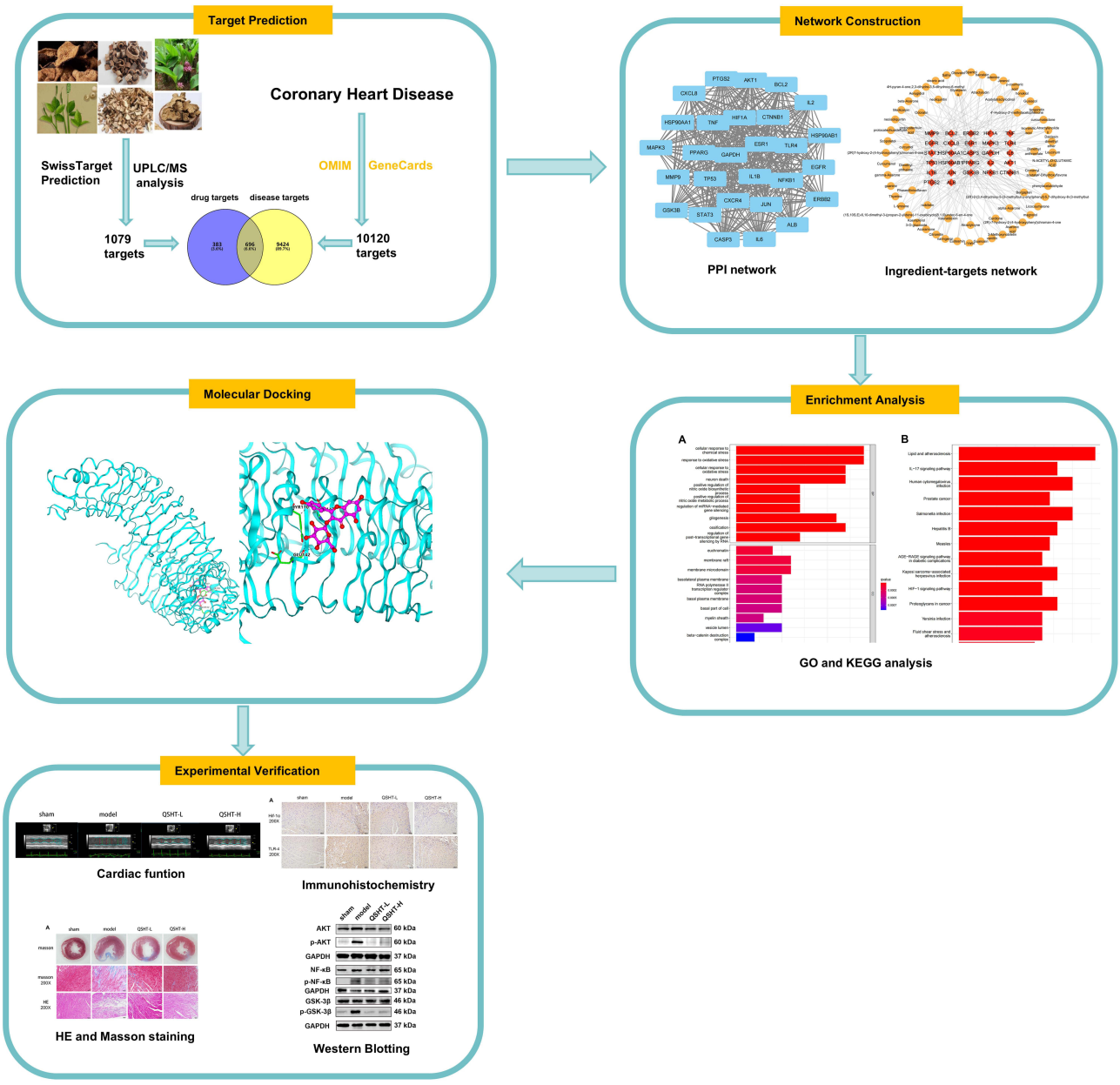

Figure 1 Flowchart of the study.

Drug Preparation

A dose of QSHT consists of rhizoma atractylodis (20 g), Magnolia officinalis (20 g), dried orange peel (10 g), Rhizoma Curcumae (15 g), Acorus gramineus (15 g) and Rhizoma Pinelliae Praeparata (15 g). Eight doses of QSHT were immersed with 8-fold water for 30 min, then decocted twice of 45 min for each time. All QSHT decoctions were combined and condensed to approximately 160 mL using a rotary evaporator. A part of the decoction was freeze-dried to obtain powder for UPLC/MS analysis. The powder was dissolved with 50% (v/v) aqueous methanol.

Identification of QSHT Ingredients by UPLC–HRMS Analysis

Thermo Fisher Q Exactive Orbitrap LC–MS/MS equipped with electrospray ionization (ESI, Thermo Fisher Scientific, Waltham, MA, USA) in positive and negative ion modes, which was controlled by Thermo Xcalibur 3.0.63 (Thermo Fisher Scientific).

An ACQUITY UPLC BEH C18 column (100 mm × 2.1 mm, 1.7 μm) was used to separate the sample with the temperature set at 40 °C. Mobile phase A was H_2O with 0.1% formic acid, and mobile phase B was 100% acetonitrile with a flow rate of 0.3 mL/min. The gradient was set as follows: 0–1 min (5% B); 1–20 min (5% B-15% B); 20–50 min (15–75% B); 50–60 min (75–95% B), 60–70 min (95% B), 70–75 min (95–5% B), The injection volume was established as 2 μL.

Full MS and data-dependent tandem mass spectrometry 2 ($ddMS^2$) in both positive and negative ion mode were used to acquire full scan MS and MS data from the samples. The scan mass range 100 to 1500 Da was selected. High resolution full-scan MS and MS^2 data were collected at resolving power of 70,000 and 17,500, respectively. The HCD collision energy was set to 10, 20, 40%. The capillary temperature was set at 300 °C, and the spray voltage was 3.0 kV for negative ion mode and 3.4 kV for positive ion mode. The flow rates of the sheath gas (N_2) and the auxiliary gas (N_2) were 50 and 10 arb, respectively. The data obtained were analyzed by Thermo Xcalibur 4.0.27 Qual Browser (Thermo Fisher Scientific).

After collecting MS and MS/MS data from the QSHT test solution, structural characterization and confirmation of QSHT constituents were performed using Compound Discoverer 3.1 software (Thermo Fisher Scientific). The main parameters of this software were set as follows: alignment retention times, maximum shift 2 min; mass tolerance, 5 ppm; detect compound, mass tolerance 5 ppm; intensity tolerance, 30%; minimal peak intensity, 500,000; data sources, mzCloud, mzVault, MassList, and ChemSpider Search; and *S*/*N* threshold, 3, after which compounds searching and matching were conducted. Then the software search report was combined with the fragmentation rule of reference MS as well as the corresponding characteristic fragment ion information.

Collection of Drug Targets and CHD Targets

After achieving the active ingredients of QSHT by UPLC/MS analysis, the sdf structures of the ingredients were downloaded from Pubchem (http://pubchem.ncbi.nlm.nih.gov), then the sdf formats of the active ingredients were uploaded into the SwissTargetPrediction database (http://www.swisstargetprediction.ch/) to predict the targets.

The Genecards database (https://www.genecards.org/) and OMIM (https://omim.org) were searched with the keyword of "coronary heart disease" to obtain disease targets.

Construction of the PPI Network with Active Ingredients-Target

Active ingredient and disease targets were imported to the Venny 2.1.0 mapping platform (http://bioinfogp.cnb.csic.es/tools/venny/) to filter shared targets. The PPI, protein-protein interaction, of every target was generated through the STRING database (https://string-db.org/). The active ingredients target network was constructed with Cytoscape software (v3.8.2) and the CytoNCA (v2.1.6) plugin was used to filter the core targets.

GO and KEGG Enrichment Analyses

To achieve the potential mechanism of QSHT in the treatment of CHD. GO and KEGG enrichment analysis was performed using the ClusterProfiler data package of R software. $P < 0.05$ indicated that the enrichment was statistically significant. Pathways with low P-values were selected for experimental verification.

Molecular Docking

The protein structures and 3D structures of the QSHT ingredients were retrieved from the RCSB Protein Data Bank and Pubchem, respectively. Molecular Docking calculations were performed on the Yinfo Cloud Platform (https://cloud.yinfotek.com). The Dock6.9 program was used to perform flexible docking and the grid scoring evaluated affinities.

Animal Experiments

Male $ApoE^{-/-}$ mice (6–8 weeks of age) and male wild-type C57BL/6 (C57) mice were obtained from the Guangdong Yaokang Biotechnology Company. All animal experiments were carried out in accordance with the Experimental Animal Use Ethics Committee of the Guangdong Hospital of Traditional Chinese Medicine (Approval No. 2022125). All animal experimental procedures were conducted in accordance with the Guidelines for the Care and Use of Laboratory Animals

published by the Ministry of Science and Technology of China. ApoE$^{-/-}$ mice were fed a high-fat diet for 2 months, and wild-type C57 mice were only fed a chow diet. All ApoE$^{-/-}$ mice were performed by ligating the left coronary artery anterior descending branch (LAD). In briefly, male ApoE$^{-/-}$ mice were anesthetized and received small animal ventilator (Rovent Jr, Kent Scientific, America) at a respiratory rate of 39 mL/min. After the pericardium was separated, the heart was exposed and the left branch of the coronary artery was ligated with a 8–0 nylon silk suture below the level of the left auricle. The sham group C57 mice (Sham, n =10) underwent the same procedure without ligation of the left coronary artery. Then, ApoE$^{-/-}$ mice were randomly divided into three groups: the MI group, the MI+QSHT -L group (low dose) and MI+QSHT -H group (high dose). ApoE$^{-/-}$ mice in the MI + L group and the MI + H group were administered the equivalent clinical dose in humans and 2 times the clinical dose of QSHT for 4 weeks. Those in the sham group and the MI group were treated with the same dose of water for 4 weeks.

Echocardiogram

Serial echocardiography was performed using a high-resolution echocardiographic system (Vevo 2100; VisualSonics Inc, Canada). All mice were lightly anesthetized with isoflurane. Transthoracic echocardiography was performed with a 18-38 MHz phased array probe. The ejection fraction (EF), fractional shortening (FS), left ventricular end-systolic dimension (LVED), and left ventricular end-systolic volume (LVEV) were measured and calculated from the M-mode recordings. The M-mode recordings were performed at the level of the papillary muscles.

HE and Masson Staining

Staining with hematoxylin-eosin (HE) and masson's trichrome (Masson) was performed to evaluate the morphological changes of the ventricles. After deparaffinization of the sections, all procedures were performed with the HE and Masson kit. The stained sections were then observed under a microscope (BX53+DP72, Olympus, Japan) and quantified with ImageJ software.

Immunohistochemistry Staining

After the sections were deparaffinized, sodium citrate buffer high-pressure boiling method was used for antigen retrieval. After washing with PBS 3 times, the sections were blocked with bovine serum albumin for 45 min. The sections were then incubated with primary antibody against TLR4 or HIF-1α overnight at 4 °C followed by incubation with horseradish peroxidase (HRP) conjugated secondary antibody. After washing with PBS 3 times, the cell nucleus was incubated with hematoxylin at room temperature for 3 min. After staining, the sections were observed under a microscope (IX51, Olympus Corporation, Tokyo, Japan) and positive areas were quantified with ImageJ software.

Western Blotting

The procedures for protein preparation and Western blot were performed as described in our previous studies.[10] In briefly, the total protein of the infarct border zone was extracted by RIPA lysis buffer with a protease and phosphatase inhibitor cocktail. Protein concentrations were determined by the instruction of the BCA assay kit. Protein samples were separated by 10% SDS-PAGE gel and then transferred to polyvinylidene fluoride (PVDF) membranes. After blocking with skim milk for 1 h, PVDF membranes were labeled with primary antibodies against AKT (CST,1:1000), p-AKT (CST,1:1000), GSK-3β (CST,1:1000), p-GSK-3β (CST,1:1000), NF-κB (CST,1:1000), p- NF-κB (Santa Cruz, 1:100), and GAPDH (CST,1:8000) followed by horseradish peroxidase (HRP) conjugated secondary antibody (CST, 1:2000). The signals of the Western blot bands were detected by Enhanced Chemiluminescence Plus. Bands quantification was carried out by Image J (NIH, USA). The protein was normalized with GAPDH.

Statistical Analysis

Data were expressed as mean ± standard deviation of mean and all experiments in this study were replicated independently at least three times. SPSS Statistics 26 was used to analyze all data. The analysis of variance (ANOVA) test was performed to determine statistical significance for multiple comparisons with LSD (equal variance) or Dunnett (unequal variance). A P value <0.05 was considered statistically significant.

Results

UPLC/MS Analysis of the Chemical Constituents of QSHT

To identify the components of QSHT decoction, the test solution was analyzed by UPLC/MS. As shown in Figure 2 and Supplementary Table S1, a total of 68 significant constituents were found in the QSHT test solution.

Targets of QSHT in Treatment of Coronary Heart Disease

As a result, a total of 1079 drug targets were obtained from the SwissTargetPrediction database, and a total of 10120 target for coronary heart disease were obtained after the duplicate targets were excluded. Finally, 696 common genes were identified by Venn analysis (Figure 3A).

Network Construction

Based on a string database, the PPI network was constructed using cytoscape software, which consisted of 731 nodes. Core targets were selected through a filter. The CytoNCA (v2.1.6) plug-in and 28 nodes were obtained (Figure 3B). The top 28 core targets based on the degree are listed in Table 1. NF-κB, TLR4, AKT1, TNF, IL-6, CASP3, GSK-3β and HIF-1α were closely related to oxidative stress and inflammation. To clarify the relationship among the ingredients of QSHT and core targets, an ingredient - targets network were constructed by Cytoscape, which comprised 96 nodes (28 core targets and 68 active ingredients) and 257 edges (Figure 3C).

Go Enrichment and KEGG Pathway Analysis

The GO enrichment and KEGG pathway analysis were employed by the R software Cluster Profiler package. As a result, 2122 BP entries, 56 CC entries, and 136 MF entries were selected. In the BP category, the core targets are mostly enriched in cellular response to chemical stress, response to oxidative stress, and neuron death (Figure 4A). A total of 147 pathways were significantly enriched ($p<0.05$). The top 20 pathways are shown in Figure 4B. Lipid and atherosclerosis, the IL-17 signaling pathway, and the HIF-1 signaling pathway were the major pathways.

Molecular Docking Analysis

To evaluate the affinities between the QSHT ingredients and the core targets, AKT1, HIF-1α, GSK-3β, TLR4 and NF-κB was used to perform molecular docking. The results are shown in Table 2 and Figure 5. Generally speaking, the grid score lower than −70 kcal/mol indicated that the component could strongly bind to the protein, the grid score is between −40 kcal/mol and −70 kcal/mol indicated that the binding force is moderate. According to the results, AKT1, HIF-1α, GSK-3β and NF-κB had a lower grid score (lower than −60 kcal/mol), among them, AKT1 and NF-κB had the strongest

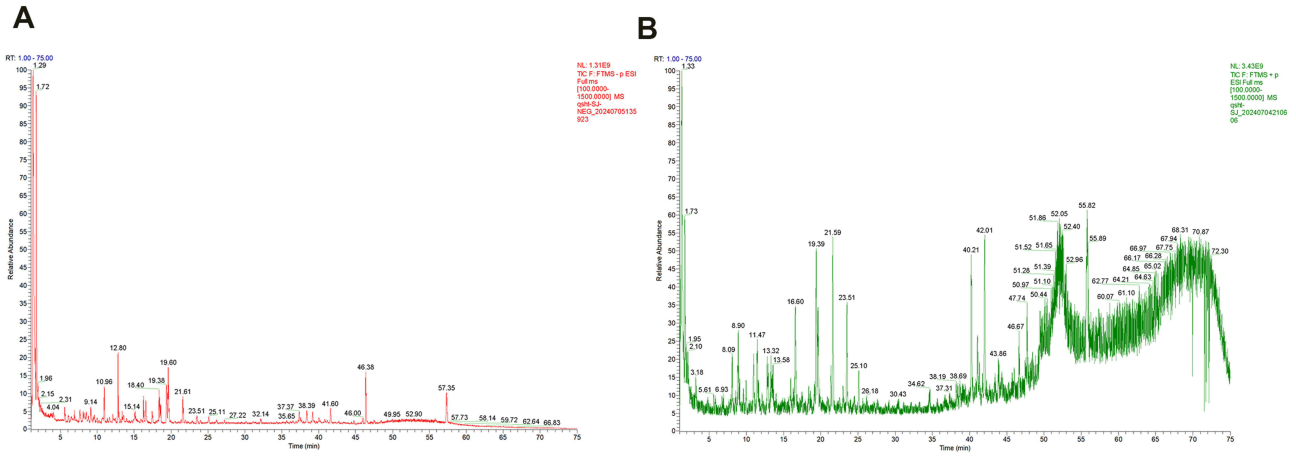

Figure 2 Analysis of QSHT components in the test solution by UPLC/MS.;(**A**) Negative ion mode total ion current chromatogram; (**B**) Positive ion mode total ion current chromatogram.

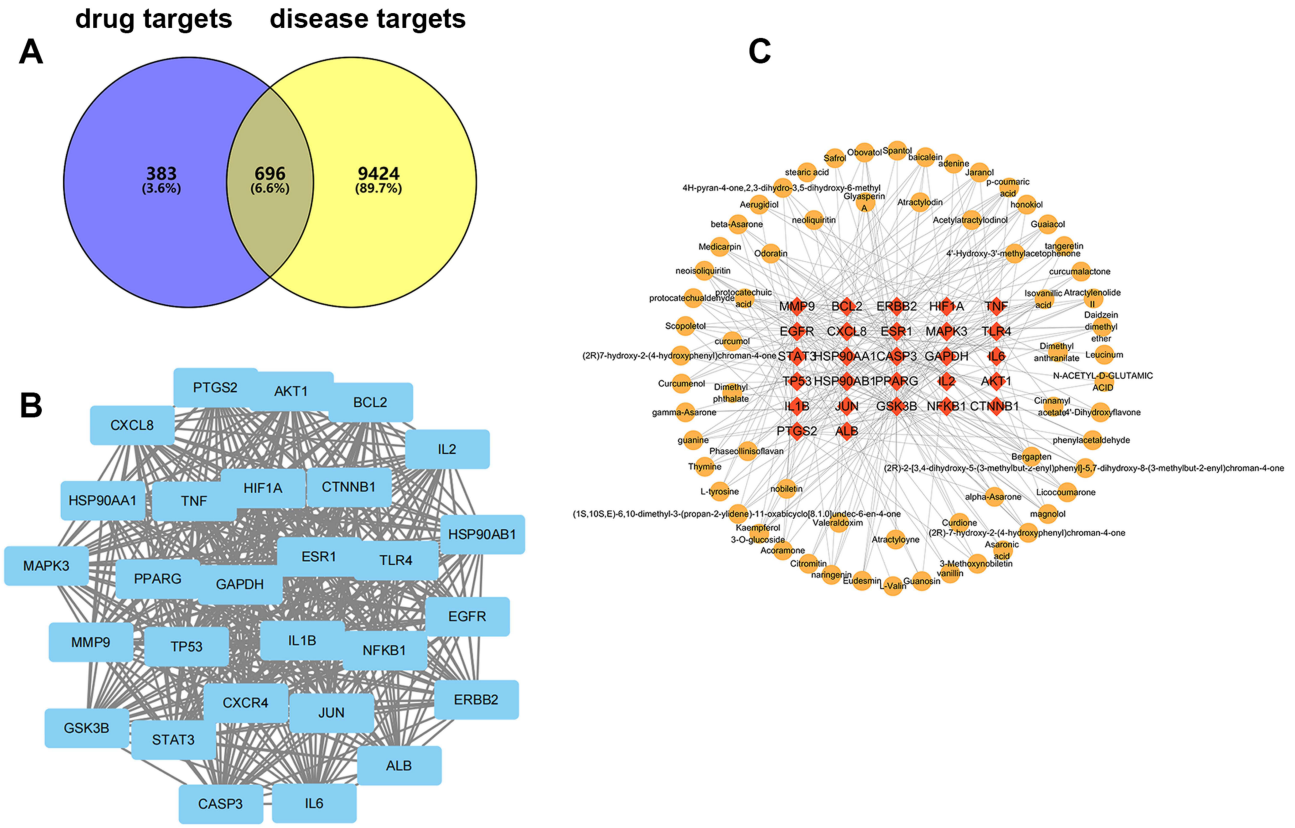

Figure 3 Identification of therapeutic targets for QSHT against CHD. (**A**) Venn diagram of targets of QSHT in treating CHD. (**B**) Protein-protein interaction network of QSHT targets against CHD. (**C**) The ingredient-targets network of QSHT. Red represents core targets, and Orange represents ingredients.

binding with the active ingredients of QSHT (lower than −70 kcal/mol), suggesting that they could be crucial targets for the treatment of CHD by QSHT. Besides, we re-docked validation with co-crystallized ligands to confirm the protein selection and molecular docking method are corrected, the results are shown in Table S2 and Figure S1, all of grid scores are lower −57 lower kcal/mol.

Table 1 The Core 28 Targets Were Identified by PPI Network Analysis

ID	Name	Closeness	Degree	Betweenness
1	NF-κB	0.579825258	214	4460.901857
2	MAPK3	0.584467574	221	7488.629702
3	STAT3	0.600328947	252	7218.378891
4	TP53	0.628227194	303	16,980.22267
5	ERBB2	0.561970747	176	3247.000964
6	EGFR	0.604805302	258	11,988.9753
7	ALB	0.615514334	278	17,798.98569
8	CASP3	0.591572123	234	6122.533773

(*Continued*)

Table 1 (Continued).

ID	Name	Closeness	Degree	Betweenness
9	GSK-3β	0.555978675	162	3677.046006
10	HSP90AA1	0.586345382	224	6794.290046
11	PTGS2	0.573448547	197	7445.359725
12	JUN	0.58681672	227	4918.974036
13	HSP90AB1	0.569422777	193	4440.762878
14	MMP9	0.5703125	196	4055.265685
15	GAPDH	0.650623886	340	28,920.38635
16	BCL2	0.588235294	225	5699.181713
17	IL6	0.637554585	318	17,790.31023
18	TNF	0.638670166	321	19,769.03815
19	ESR1	0.590614887	231	10,077.31781
20	HIF-1α	0.581673307	218	4758.207149
21	AKT1	0.651204282	342	24,922.59837
22	CTNNB1	0.598360656	250	11,071.53655
23	PPARG	0.583067093	217	9781.200496
24	CXCR4	0.549285177	156	3620.508434
25	IL2	0.545590433	141	3373.502238
26	IL1β	0.618120237	283	13,608.33453
27	TLR4	0.557251908	173	3201.724218
28	CXCL8	0.561970747	181	4718.059536

QSHT Improves Cardiac Function

We explored the effect of QSHT on coronary heart disease in Apoe$^{-/-}$ mice (Figure 6A). All mice were conducted echocardiogram tests at the end of 12 weeks. Compared to the Sham group, EF and FS decreased remarkably in the model group after 12 weeks, meanwhile, LVEDS and LVEVS increased significantly. These indicate heart dysfunction after MI in high-fat diet fed ApoE$^{-/-}$ mice. On the contrary, the low and high dose of QSHT significantly improved these heart dysfunctions and dramatically improved EF and FS, and significantly decreased LVDS and LVEVS (Figure 6B–F).

QSHT Attenuated Myocardial Inflammation and Fibrosis

Normally, cardiac dysfunction is related to cardiac hypertrophy. Compared to the Sham group, the model group had an increased ratio of heart weight to body weight, which was substantially attenuated by the low and high dose of the QSHT group (Figure 7B). The protection of QSHT was further confirmed by HE staining and Masson staining of the heart section. The results of HE staining indicate severe inflammatory cell infiltration and myocardial structural disorder in the model group, while low and high doses of QSHT could reduce the infiltration of inflammatory cells, indicating that QSHT could protect the heart by anti-heart inflammation (Figure 7A). The results of masson trichrome staining showed significant collagen deposition in the model group. While the low and high doses of QSHT markedly

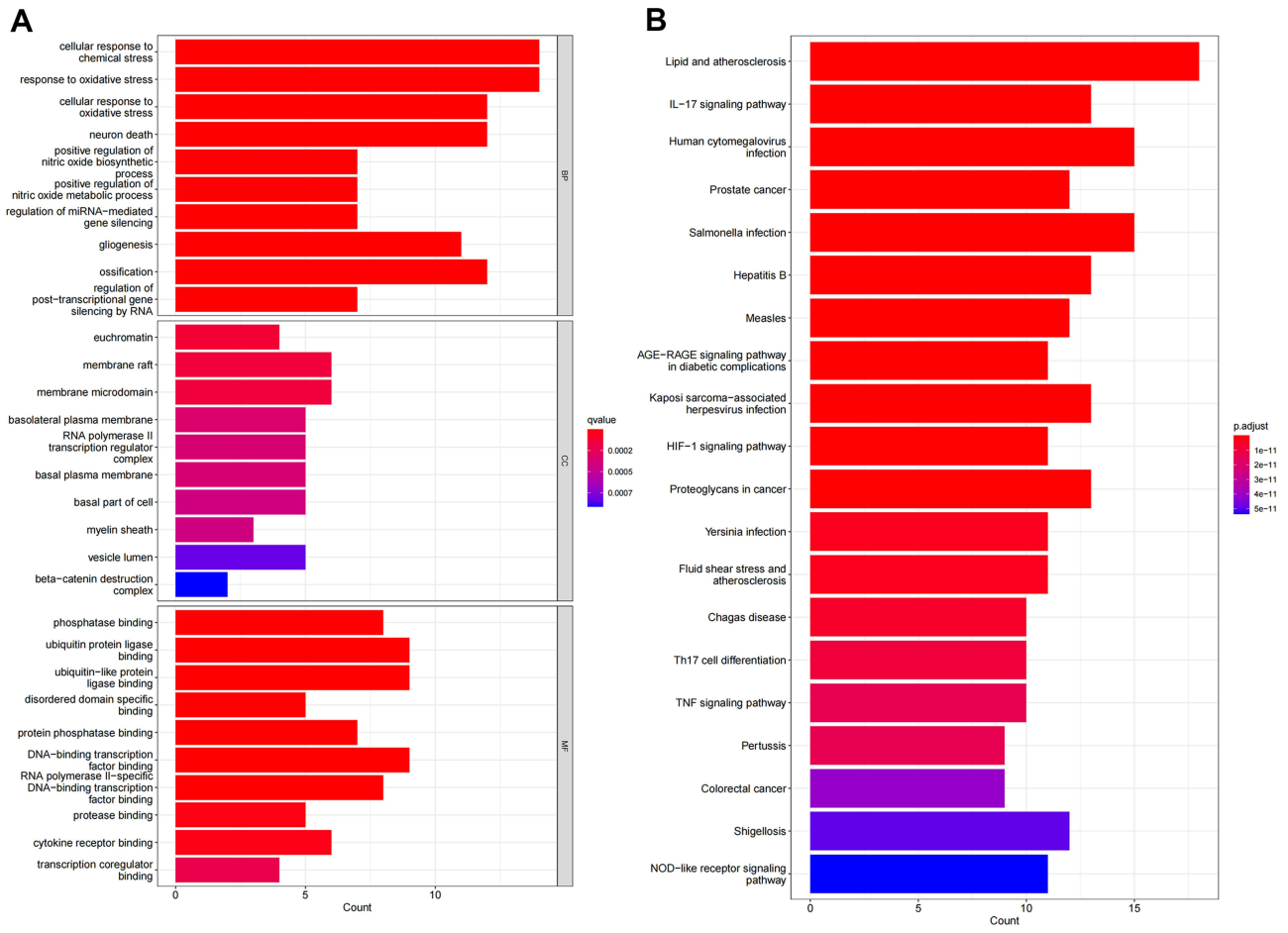

Figure 4 Analysis of core targets. (**A**) GO enrichment analysis: the top 30 terms of biological process (BP), cellular component (CC), and molecular function (MF) with P<0.05. (**B**) KEGG pathways analysis: the top 20 terms of KEGG enrichment pathway with P<0.05.

reduced myocardial interstitial fibrosis (Figure 7A and C). Those data demonstrated that QSHT substantially protects ApoE$^{-/-}$ mice against high-fat diet and MI-induced myocardial injury.

QSHT Regulated the TLR4/NF-κB and AKT/HIF-1α Singnaling Pathway in ApoE$^{-/-}$ Mice

Based on network pharmacology and molecular docking, TLR4/NF-κB and AKT/HIF-1α singnaling pathway might be the major pathways. To verify the mechanisms of QSHT reduced heart injury, we performed Western Blot and immunohistochemistry to detect protein expression of key targets of TLR4/NF-κB and AKT/HIF-1α pathway.

Table 2 The Top 20 Affinities Between the QSHT Ingredients and the Core Targets

Protein	PDB ID	Ingredient	Grid_Score	Grid_vdw_energy	Grid_es_energy
AKT1	7NH5	Kaempferol 3-O-glucoside	−84.127327	−71.98175	−12.145575
AKT1	7NH5	Nobiletin	−77.258522	−74.174805	−3.083716
AKT1	7NH5	3-Methoxynobiletin	−76.728806	−72.86142	−3.867388
NF-κB	4DN5	Kaempferol 3-O-glucoside	−74.227707	−64.57708	−9.650623
AKT1	7NH5	Citromitin	−73.482613	−71.263924	−2.21869

(*Continued*)

Table 2 (Continued).

Protein	PDB ID	Ingredient	Grid_Score	Grid_vdw_energy	Grid_es_energy
NF-κB	4DN5	Citromitin	−71.091789	−63.366093	−7.725697
NF-κB	4DN5	Nobiletin	−69.21209	−67.005142	−2.206944
HIF-1α	4W9C	Kaempferol 3-O-glucoside	−68.714775	−60.807777	−7.906997
AKT1	7NH5	Tangeretin	−67.913956	−65.272972	−2.640984
AKT1	7NH5	Eudesmin	−67.462273	−67.145103	−0.317172
NF-κB	4DN5	Tangeretin	−67.433243	−60.033005	−7.400235
GSK-3β	7U2Z	Kaempferol 3-O-glucoside	−66.986504	−57.217945	−9.768558
NF-κB	4DN5	3-Methoxynobiletin	−66.549957	−67.019318	0.469361
NF-κB	4DN5	Eudesmin	−65.311493	−63.570854	−1.740641
AKT1	7NH5	Atractyloyne	−65.015121	−55.027584	−9.987539
HIF-1α	4W9C	Citromitin	−63.855148	−59.649502	−4.205647
HIF-1α	4W9C	Nobiletin	−63.599915	−60.48127	−3.118645
NF-kB	4DN5	Atractyloyne	−62.224304	−56.588825	−5.635478
HIF	4W9C	3-Methoxynobiletin	−61.258972	−60.196419	−1.062554
GSK	7U2Z	3-Methoxynobiletin	−60.079407	−58.328854	−1.750553

Compared to the sham group, the expression of TLR4, p-NF-κB, p-AKT, HIF-1α and p-GSK-3β was increased in the model group, while the tendency could be reversed by a low and high dose of QSHT (Figures 8 and 9).

Discussion

As the top of traditional Chinese cultural treasures, TCM has particular advantages in the treatment of CHD. In recent years, great progress has been made in the treatment of CHD, which can effectively improve the cardiac function of patients and enhance the quality of life of patients.[11] The QSHT decoction was developed by the famous TCM expert of Keji Chen based on Pingwei San. A recent study showed that Pingwei San improved chronic colitis in mice by suppressed NF-κB pathway and NLRP3 inflammasome activation.[12] However, the effect and mechanism of QSHT or Pingwei San on CHD remain unknown. In the present study, we performed network pharmacology analysis and related experimental verification to study the effect and mechanism of QSHT on CHD. The major results are as follows: (1) Active ingredients of QSHT decoction were screened through UPLC/MS, which target a total of 1079 genes. Cross-contrasting the disease targets and the ingredients targets resulted in 696 common genes. (2) Go and KEGG enrichment analysis revealed that the anti-inflammatory and anti-oxidation of QSHT might be the main mechanisms in CHD. Among them, TLR4/NF-κB and AKT/HIF-1α signaling pathways might be the key pathways for the anti-inflammatory and anti-oxidation action of QSHT. (3) The key genes of the network include NF-κB, TLR4, AKT1, GSK-3β and HIF-1α. Furthermore, molecular docking verified the affinities between the ingredients of QSHT and those core targets. (4) Animal experimental results demonstrated that QSHT improved cardiac function, attenuated myocardial inflammation, and cardiac fibrosis after MI in $ApoE^{-/-}$ mice. (5) QSHT improved cardiac function might be through regulating TLR4/NF-κB and AKT/HIF-1α signaling pathways.

In the drug-ingredient-target network, Atractylenolide II, honokiol, magnolol, 3-Methoxynobiletin, naringenin, p-coumaric acid and baicalein have more therapeutic targets for CHD than other ingredients, therefore, those

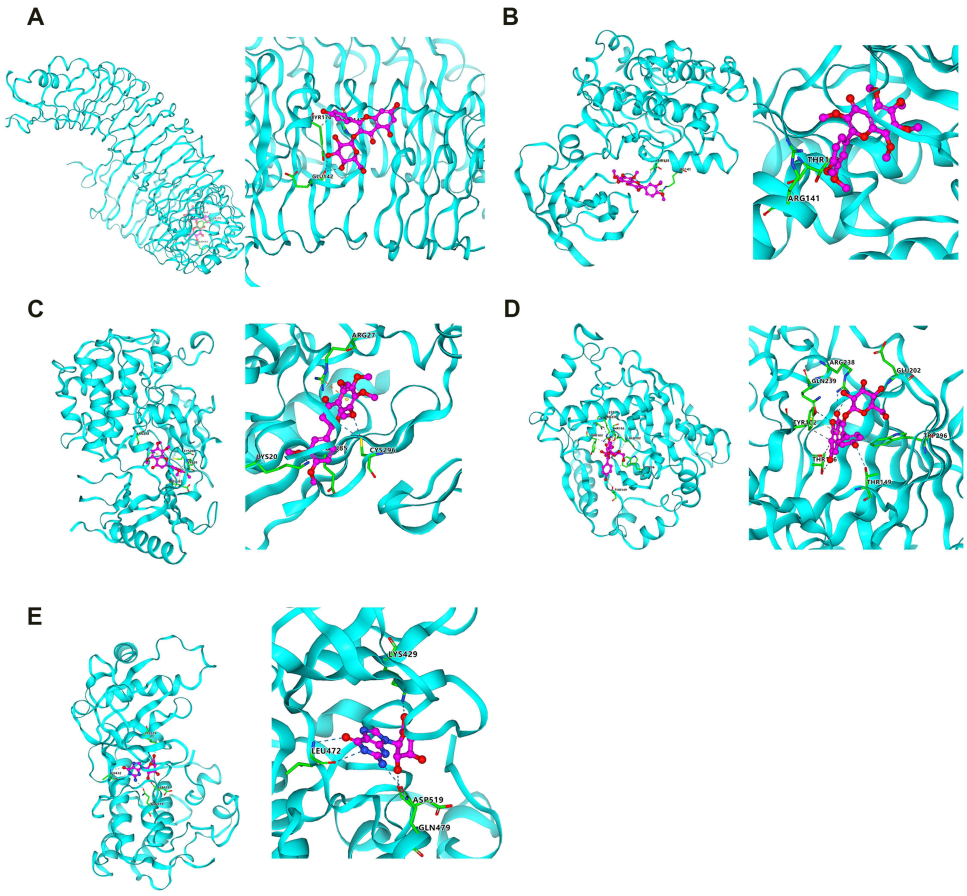

Figure 5 Docking patterns of ingredients of QSHT and target proteins. (**A**) Kaempferol 3-O-glucoside and TLR4. (**B**) 3-Methoxynobiletin and GSK-3β. (**C**) Citromitin and AKT1. (**D**) Kaempferol 3-O-glucoside and HIF-1α. (**E**) Guanosin and NF-κB.

ingredients might be the core effector components of QSHT in treatment of CHD. Atractylenolide II is the main ingredient in rhizoma atractylodis, researches have shown that atractylenolide II has remarkable anti-cancer, anti-fibrosis and anti-oxidation activities.[13–15] It showed a significant antitumor effect through elevated anti-inflammatory activity by inhibiting the NF-κB pathways and modulating AKT/ERK signaling pathways.[16,17] Furthermore, Atractylenolide II could improve cardiac function in spontaneous hypertensive rats by attenuating cardiac fibrosis and oxidative stress.[14] Honokiol and magnolol are compounds of magnolia officinalis. Recently, research has shown that honokiol and magnolol could suppress tumor, alleviate oxidative stress, fibrosis, and inflammation as well as protect nerve.[18–22] Samant et al showed that honokiol blocks cardiac hypertrophic and cardiac fibrosis via activating sirt3.[19] Magnolol mediated biological functions implicated many signaling pathways, such as the NF- κB/MAPK, Nrf2/HO-1, and PI3K/AKT pathways.[23] 3-Methoxynobiletin could alleviate obesity induced by a high-fat diet, lower blood triglyceride, total cholesterol and low-density lipoprotein.[24] Naringenin could prevent nonalcoholic fatty liver disease via down-regulating NLRP3/NF-κB pathway, then reducing inflammation in mice.[25] Naringenin could also have significant therapeutic potential in cardiovascular disease through anti-inflammatory, anti-oxidative and anti-apoptotic activity.[26] P-coumaric acid is the main ingredient of dried orange peel and Rhizoma Pinellinae Praeparata, it has many pharmacological activities, including antioxidant, inhibiting lipid peroxidation, immune regulation and anti-inflammatory action.[27–29] P-coumaric acid could also protect cardiomyocytes by regulating macrophage polarization and inhibiting inflammation in myocardial ischemia/reperfusion mice.[30] Baicalein could attenuate isoproterenol-induced cardiac hypertrophy by clearing reactive oxygen species and promoting autophagy by binding to the transcription factor FOXO3a.[31] Furthermore, recent researches have discovered several pharmacological functions of baicalein, such

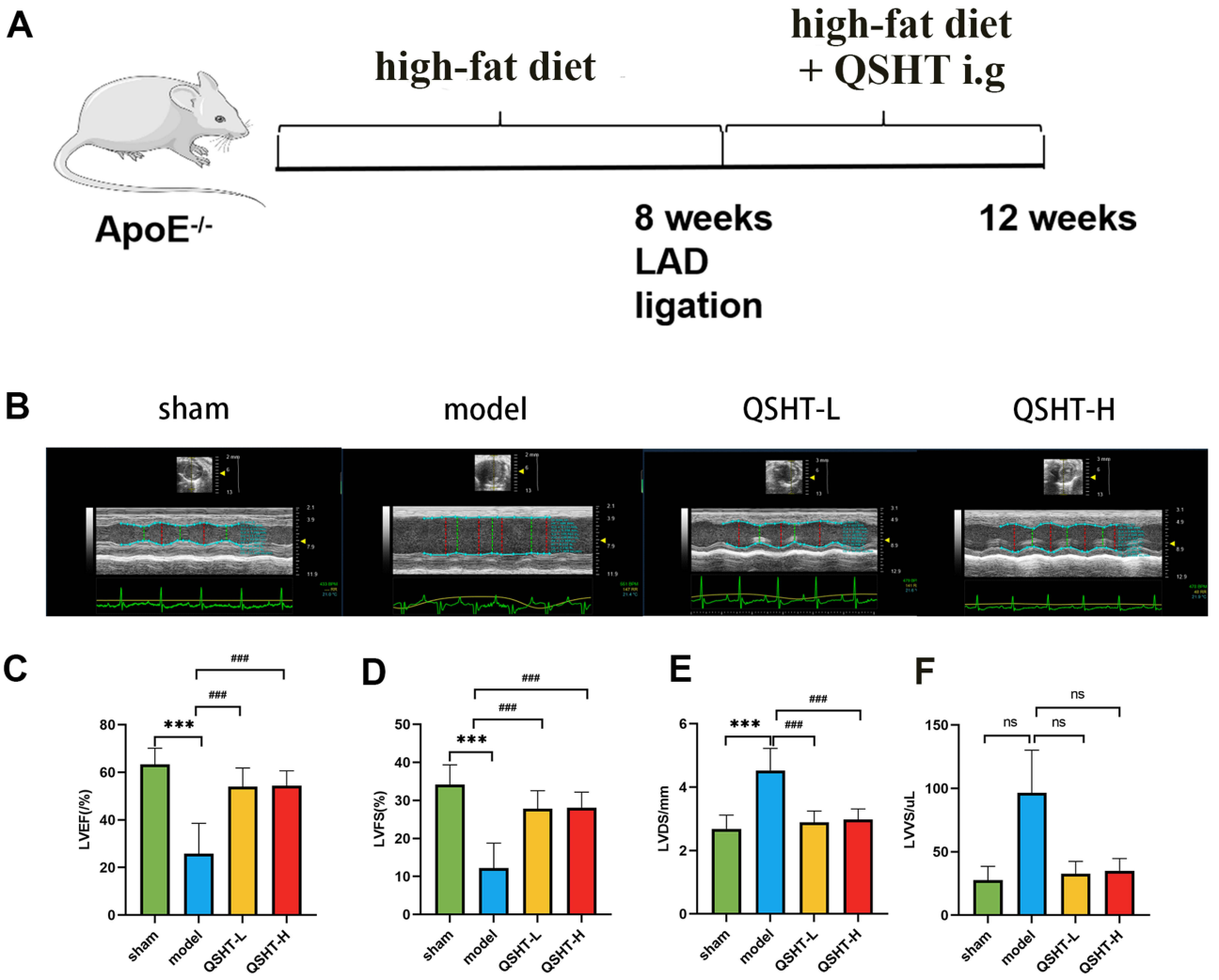

Figure 6 QSHT improved the cardiac function after MI in ApoE$^{-/-}$ mice (n=6). (**A**) Animal experimental strategy. ApoE-/- mice aged 8 weeks were high fat diet-fed (HFD)for 8 weeks. At the end of the 8-week period, myocardial infarction model was made by ligating LAD, the HFD continued and treated with QSHT decoction or vehicle (water) for the next 4 weeks. (**B**) Representative images of M-mode echocardiograms. (**C**) Statistical results of EF. (**D**) Statistical results of FS. (**E**) Statistical results of LVEDS. (**F**) Statistical results of LVEVS. ***P<0.001vs sham group;###P<0.001 vs model group.

as antioxidant, anti-cancer and anti-inflammatory effects.[32,33] Recently, baicalein has been shown to protect the heart and attenuate cardiac hypertrophy involved several signaling pathways, such as AKT/mTOR, NF-κB and calcineurin signaling pathway.[34] All in all, those active ingredients have potent anti-inflammatory and antioxidant activity, therefore, they might be the key components of QSHT in the treatment of CHD. Furthermore, Atractylenolide II, honokiol and magnolol,[35] Naringenin[36] and baicalein[31] could improve cardiac function in different pathological model, they may become novel therapeutics with a better effect than QSHT, we will take further experiments to prove their effect on CHD in future.

Go enrichment analysis showed that QSHT treats CHD by regulating biological responses such as oxidative stress, chemical stress, and neuron death. KEGG enrichment analysis results showed that lipid and atherosclerosis, the IL-17 signaling pathway and the HIF-1 signaling pathway may be the potential key pathway of QSHT in the treatment of coronary heart disease.

Previous studies have shown that disturbed lipid metabolism, increased oxidative stress, and inflammation are associated with the occurrence and development of CHD.[37,38] TLR4 plays a key role in facilitating the inflammatory response during heart disease. The expression of TLR4 and NF-κB was increased in the heart of MI mice.[39] Treatment with TLR4 inhibitor significantly reduced the size of the infarct area and improved cardiac

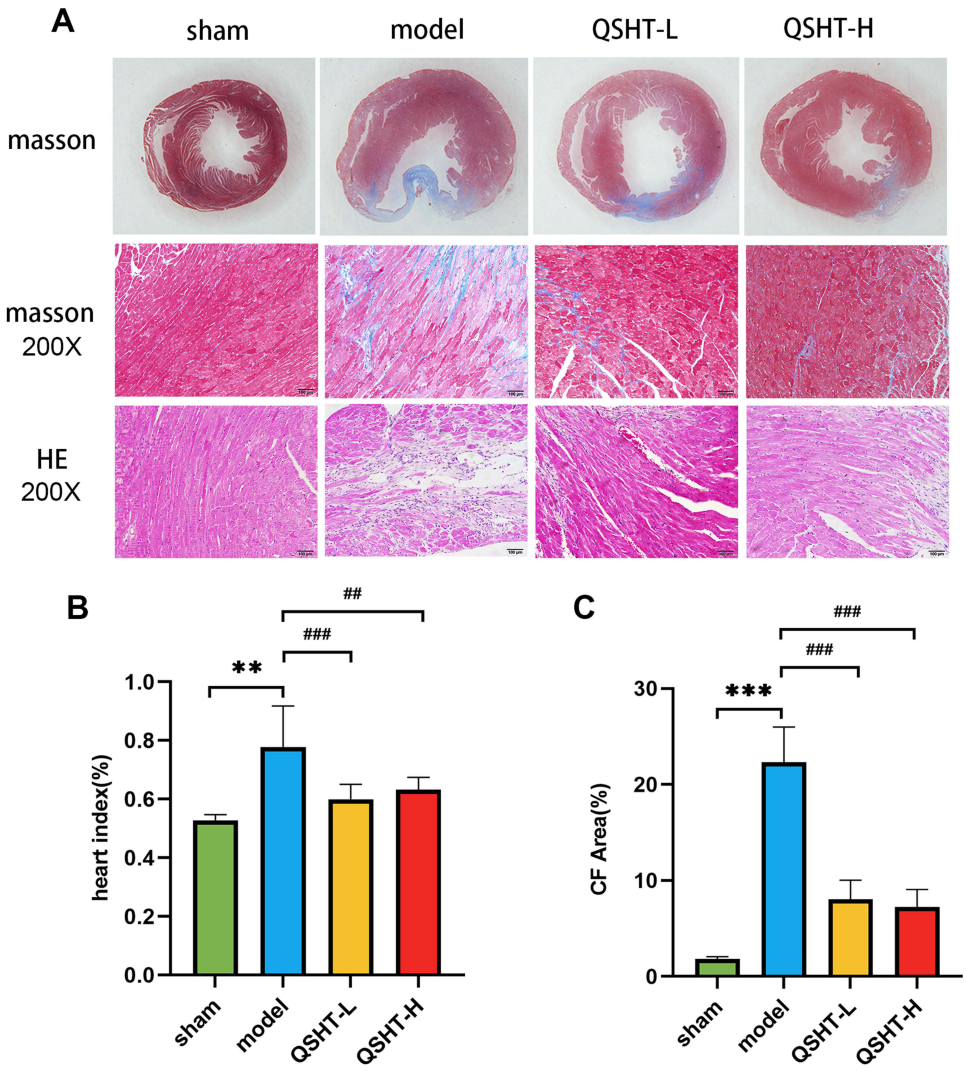

Figure 7 QSHT attenuated cardiac fibrosis and inflammation after MI in ApoE$^{-/-}$ mice (n=6). (**A**) Representative images of Masson's staining and HE staining; (**B**) Statistical results of heart index. (**C**)Statistical results of cardiac fibrosis. **P<0.01, ***P<0.001vs sham group; ##P<0.01, ###P<0.001 vs model group.

function in MI mice.[40] Furthermore, inhibition of TLR4/NF-κB pathway could regulate lipid peroxidation and inflammasome activation in high-fat diet-fed golden hamsters.[41] HIF-1α has been shown to play an important protective role in the pathophysiological progress of ischemic heart disease.[42] HIF-1α deficiency may result in congenital heart defects in human.[43] The PI3K/AKT pathway is important for regulating HIF-1α protein levels to hypoxia, Phosphorylated AKT could regulate HIF-1α activity.[44] In the present study, we demonstrated that QSHT could improve cardiac function in CHD mice. To explore the mechanism of QSHT in the treatment of CHD, we compared the difference in protein expression of key targets in mouse hearts by Western blot and immunohistochemistry. The experimental results showed that compared to the sham group, the expression of TLR4, NF-κB, p-AKT and HIF-1α was significantly increased in the model group, while the expression of those proteins was significantly reduced in the QSHT group. Additionally, molecular docking analysis also demonstrated that AKT1, HIF-1α, GSK-3β, TLR4 and NF-κB are might be crucial targets for QSHT treating CHD. These results are in agreement with the predicted results of network pharmacology.

To our knowledge, this research is the first to study the efficacy and mechanism of QSHT in the treatment of CHD. By integrating network pharmacology and experimental verification, we demonstrated that QSHT could improve cardiac function and attenuate cardiac fibrosis by regulating TLR4/NF-κB and AKT/HIF-1α signaling

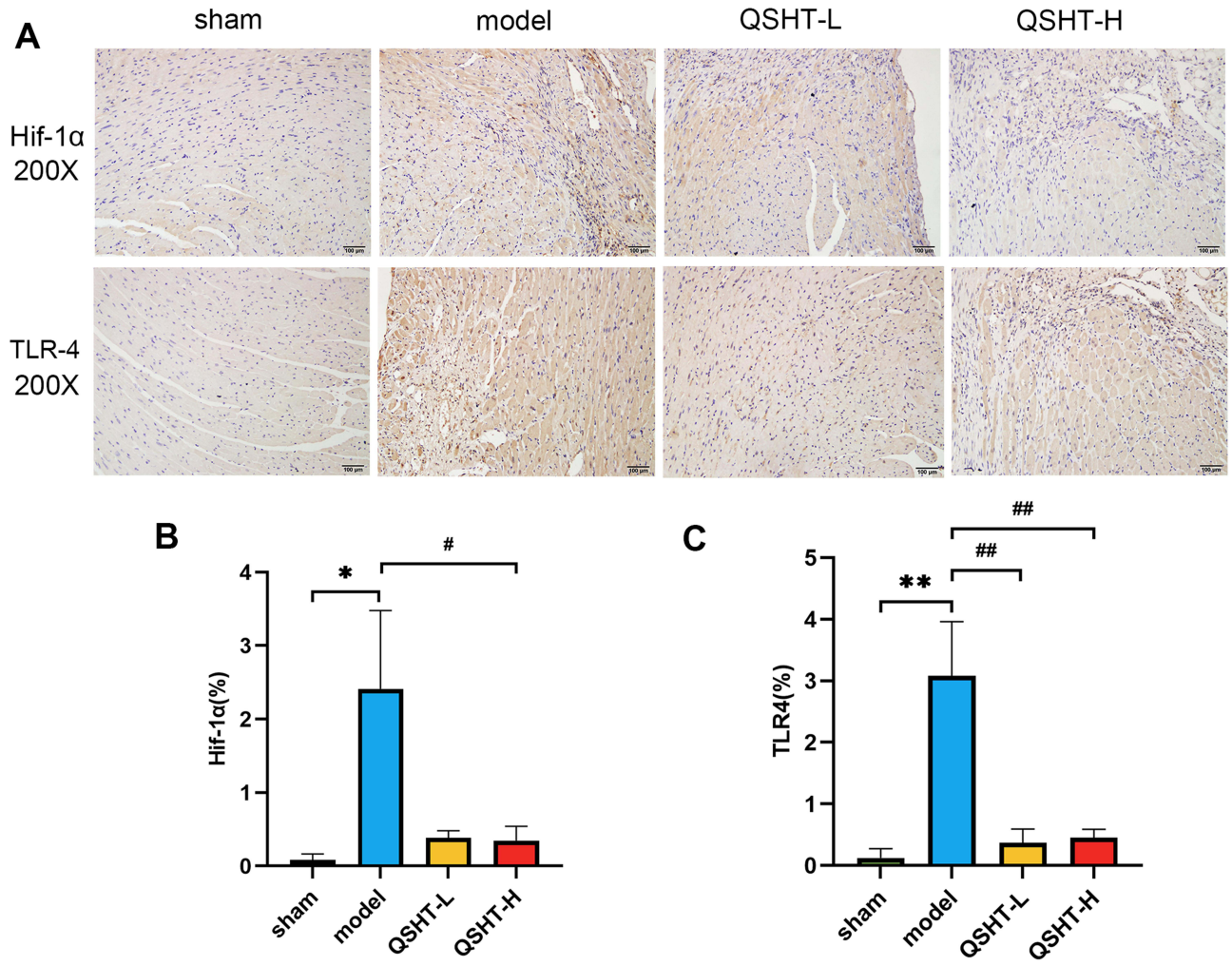

Figure 8 QSHT decreased expression of HIF-1α and TLR4 (n=5). (**A**) Representative images of Immunohistochemical. (**B**) Statistical results of expression of HIF-1α (**C**) Statistical results of expression of TLR4. *P<0.05, **P<0.01 vs sham group;#P<0.05, ##P<0.01 vs model group.

pathway after MI in ApoE$^{-/-}$ mice, suggesting its utility in the treatment of CHD. However, the key active ingredients and more detailed mechanism of QSHT in the treatment of CHD still need to be studied in further detail in future research.

Limitation

In this study, we only demonstrated that the effect and mechanism of QSHT decoction in the treatment of CHD, but not the metabolite isolation from the QSHT decoction. In future, we need to verify the effect of metabolites by vitro experiments, and compare whether those metabolites can become novel therapeutics with a better effect than QSHT.

Ethics Statement

This study is involving human data from public database OMIM and Genecards. Due to OMIM and Genecards databases are publicly accessible and users can freely download relevant data for research and publish related articles, the Ethics committee of Guangdong Hospital of Traditional Chinese Medicine confirms that the need for ethics approval for the aspect of this study involving public database has been waived.

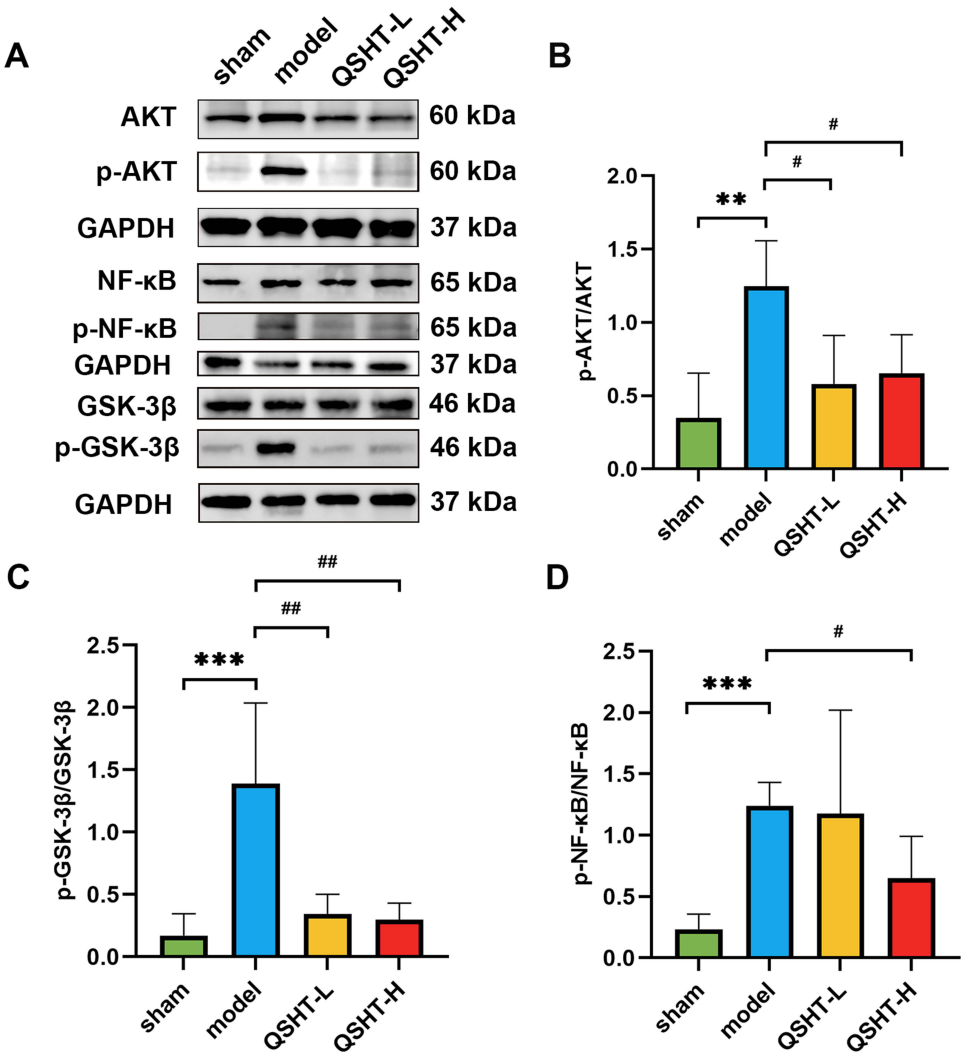

Figure 9 The Effect of QSHT on expression of AKT, GSK-3β and NF-κB (n=5).The expression of AKT, GSK-3β, NF-κB phosphorylation by Western blot. (**B–D**) Statistical results of p-AKT/AKT, p-GSK-3β/GSK-3β and p-NF-κB/NF-κB. ***P<0.001, **P<0.01 vs sham group; #P<0.05, ##P<0.01 vs MI group.

Funding

The present work was supported by Guangzhou Basic and Applied Basic Research Foundation (Grant Nos. 202201020348, 202201020488, and 2023A03J0742), National Natural Science Foundation of China (Grant No. 82074369), the Specific Fund of State Key Laboratory of Dampness Syndrome of Chinese Medicine (Grant Nos. SZ2021ZZ46, SZ2021ZZ12, SZ2021ZZ26, SZ2021ZZ33, SZ2023ZZ13 and SZ2022KF23), and the Traditional Chinese Medicine Bureau of Guangdong Province (Grant No. 20225019), Natural Science Foundation of Guangdong Province (Nos. 2022A1515010103, and 2023B1212060063).

Disclosure

The authors report no conflicts of interest in this work.

References

1. Li H, Sun K, Zhao R, et al. Inflammatory biomarkers of coronary heart disease. *Front Biosci*. 2018;10(1):185–196. doi:10.2741/s508
2. Wang X, Wang T, Wang Y, et al. Research progress on classical traditional Chinese medicine taohong siwu decoction in the treatment of coronary heart disease. *Biomed Pharmacother*. 2022;152:113249. doi:10.1016/j.biopha.2022.113249

3. Gao J, Pan Y, Zhao Y, et al. Network pharmacology study on molecular mechanisms of zhishi xiebai guizhi decoction in the treatment of coronary heart disease. *Evid Based Complement Alternat Med*. 2021;2021:3574321. doi:10.1155/2021/3574321
4. Dong Q, Li Z, Ji Q, et al. Editorial: inflammatory factors in coronary heart disease: mechanism, diagnosis, and therapy. *Front Cardiovasc Med*. 2023;10:1234132. doi:10.3389/fcvm.2023.1234132
5. Liang B, Qu Y, Zhao QF, et al. Guanxin V for coronary artery disease: a retrospective study. *Biomed Pharmacother*. 2020;128:110280. doi:10.1016/j.biopha.2020.110280
6. Zhong A, Wang H, Sun Y, et al. Discussion on the pathogenesis and intervention measures of phlegm and dampness constitution and chest obstruction (coronary heart disease). *Li J Tradl Chin Med*. 2017;44(06):1175–1177.
7. Zhang J, Yang Z, Jia X, et al. Integrated network pharmacology and metabolomics to reveal the mechanism of qishenyiqi dripping pills (T101) against cardiac structural and functional abnormalities. *Front Pharmacol*. 2022;13:1017433. doi:10.3389/fphar.2022.1017433
8. Luo TT, Lu Y, Yan SK, et al. Network pharmacology in research of Chinese medicine formula: methodology, application and prospective. *Chin J Integr Med*. 2020;26(1):72–80. doi:10.1007/s11655-019-3064-0
9. Zhang R, Zhu X, Bai H, et al. Network pharmacology databases for traditional Chinese medicine: review and assessment. *Front Pharmacol*. 2019;10:123. doi:10.3389/fphar.2019.00123
10. Ma J, Yin C, Ma S, et al. Shensong Yangxin capsule reduces atrial fibrillation susceptibility by inhibiting atrial fibrosis in rats with post-myocardial infarction heart failure. *Drug Des Devel Ther*. 2018;12:3407–3418. doi:10.2147/DDDT.S182834
11. Yang X, He T, Han S, et al. The role of traditional Chinese medicine in the regulation of oxidative stress in treating coronary heart disease. *Oxid Med Cell Longev*. 2019;2019:3231424. doi:10.1155/2019/3231424
12. Zhang Z, Shen P, Xie W, et al. Pingwei San ameliorates dextran sulfate sodium-induced chronic colitis in mice. *J Ethnopharmacol*. 2019;236:91–99. doi:10.1016/j.jep.2019.01.043
13. Deng M, Chen H, Long J, et al. Atractylenolides (I, II, and III): a review of their pharmacology and pharmacokinetics. *Arch Pharm Res*. 2021;44(7):633–654. doi:10.1007/s12272-021-01342-6
14. Song X, Wang L, Liu M, et al. Atractylenolide II ameliorates myocardial fibrosis and oxidative stress in spontaneous hypertension rats. *Technol Health Care*. 2023:1–12—.
15. Xiao C, Xu C, He N, et al. Atractylenolide II prevents radiation damage via MAPKp38/Nrf2 signaling pathway. *Biochem Pharmacol*. 2020;177:114007. doi:10.1016/j.bcp.2020.114007
16. Dou S, Yang C, Zou D, et al. Atractylenolide II induces cell cycle arrest and apoptosis in breast cancer cells through ER pathway. *Pak J Pharm Sci*. 2021;34(4):1449–1458.
17. Tian S, Yu H. Atractylenolide II inhibits proliferation, motility and induces apoptosis in human gastric carcinoma cell lines HGC-27 and AGS. *Molecules*. 2017;22(11):1886. doi:10.3390/molecules22111886
18. Huang K, Chen Y, Zhang R, et al. Honokiol induces apoptosis and autophagy via the ROS/ERK1/2 signaling pathway in human osteosarcoma cells in vitro and in vivo. *Cell Death Dis*. 2018;9(2):157. doi:10.1038/s41419-017-0166-5
19. Pillai VB, Samant S, Sundaresan NR, et al. Honokiol blocks and reverses cardiac hypertrophy in mice by activating mitochondrial Sirt3. *Nat Commun*. 2015;6(1):6656. doi:10.1038/ncomms7656
20. Talarek S, Listos J, Barreca D, et al. Neuroprotective effects of honokiol: from chemistry to medicine. *Biofactors*. 2017;43(6):760–769. doi:10.1002/biof.1385
21. Chiang CK, Sheu ML, Hung KY, et al. Honokiol, a small molecular weight natural product, alleviates experimental mesangial proliferative glomerulonephritis. *Kidney Int*. 2006;70(4):682–689. doi:10.1038/sj.ki.5001617
22. Cicalau G, Babes PA, Calniceanu H, et al. Anti-inflammatory and antioxidant properties of carvacrol and magnolol, in periodontal disease and diabetes mellitus. *Molecules*. 2021;26(22):6899. doi:10.3390/molecules26226899
23. Zhang J, Chen Z, Huang X, et al. Insights on the multifunctional activities of magnolol. *Biomed Res Int*. 2019;2019:1847130. doi:10.1155/2019/1847130
24. Huang CH, Hsiao SY, Lin YH, et al. Effects of fermented citrus peel on ameliorating obesity in rats fed with high-fat diet. *Molecules*. 2022;27(24):8966. doi:10.3390/molecules27248966
25. Wang Q, Ou Y, Hu G, et al. Naringenin attenuates non-alcoholic fatty liver disease by down-regulating the NLRP3/NF-kappaB pathway in mice. *Br J Pharmacol*. 2020;177(8):1806–1821. doi:10.1111/bph.14938
26. Heidary MR, Samimi Z, Moradi SZ, et al. Naringenin and naringin in cardiovascular disease prevention: a preclinical review. *Eur J Pharmacol*. 2020;887:173535. doi:10.1016/j.ejphar.2020.173535
27. Pragasam SJ, Venkatesan V, Rasool M. Immunomodulatory and anti-inflammatory effect of p-coumaric acid, a common dietary polyphenol on experimental inflammation in rats. *Inflammation*. 2013;36(1):169–176. doi:10.1007/s10753-012-9532-8
28. Shen Y, Song X, Li L, et al. Protective effects of p-coumaric acid against oxidant and hyperlipidemia-an in vitro and in vivo evaluation. *Biomed Pharmacother*. 2019;111:579–587. doi:10.1016/j.biopha.2018.12.074
29. Huang X, You Y, Xi Y, et al. p-coumaric acid attenuates IL-1beta-induced inflammatory responses and cellular senescence in rat chondrocytes. *Inflammation*. 2020;43(2):619–628. doi:10.1007/s10753-019-01142-7
30. Li N, Guo X, Li R, et al. p-Coumaric acid regulates macrophage polarization in myocardial ischemia/reperfusion by promoting the expression of indoleamine 2, 3-dioxygenase. *Bioengineered*. 2021;12(2):10971–10981. doi:10.1080/21655979.2021.2001924
31. Liu BY, Li L, Liu GL, et al. Baicalein attenuates cardiac hypertrophy in mice via suppressing oxidative stress and activating autophagy in cardiomyocytes. *Acta Pharmacol Sin*. 2021;42(5):701–714. doi:10.1038/s41401-020-0496-1
32. Li Y, Chen Q, Ran D, et al. Changes in the levels of 12/15-lipoxygenase, apoptosis-related proteins and inflammatory factors in the cortex of diabetic rats and the neuroprotection of baicalein. *Free Radic Biol Med*. 2019;134:239–247. doi:10.1016/j.freeradbiomed.2019.01.019
33. Dai C, Tang S, Wang Y, et al. Baicalein acts as a nephroprotectant that ameliorates colistin-induced nephrotoxicity by activating the antioxidant defence mechanism of the kidneys and down-regulating the inflammatory response. *J Antimicrob Chemother*. 2017;72(9):2562–2569. doi:10.1093/jac/dkx185
34. Wang AW, Song L, Miao J, et al. Baicalein attenuates angiotensin II-induced cardiac remodeling via inhibition of AKT/mTOR, ERK1/2, NF-kappaB, and calcineurin signaling pathways in mice. *Am J Hypertens*. 2015;28(4):518–526. doi:10.1093/ajh/hpu194

35. Aktay I, Bitirim CV, Olgar Y, et al. Cardioprotective role of a magnolol and honokiol complex in the prevention of doxorubicin-mediated cardiotoxicity in adult rats. *Mol Cell Biochem*. 2024;479(2):337–350. doi:10.1007/s11010-023-04728-w
36. Li Y, He B, Zhang C, et al. Naringenin attenuates isoprenaline-induced cardiac hypertrophy by suppressing oxidative stress through the AMPK/NOX2/MAPK signaling pathway. *Nutrients*. 2023;15(6):1340.
37. Yang X, Li Y, Li Y, et al. Oxidative stress-mediated atherosclerosis: mechanisms and therapies. *Front Physiol*. 2017;8:600. doi:10.3389/fphys.2017.00600
38. Mallika V, Goswami B, Rajappa M. Atherosclerosis pathophysiology and the role of novel risk factors: a clinicobiochemical perspective. *Angiology*. 2007;58(5):513–522. doi:10.1177/0003319707303443
39. Kaczorowski DJ, Nakao A, Mccurry KR, et al. Toll-like receptors and myocardial ischemia/reperfusion, inflammation, and injury. *Curr Cardiol Rev*. 2009;5(3):196–202. doi:10.2174/157340309788970405
40. Fujiwara M, Matoba T, Koga JI, et al. Nanoparticle incorporating Toll-like receptor 4 inhibitor attenuates myocardial ischaemia-reperfusion injury by inhibiting monocyte-mediated inflammation in mice. *Cardiovasc Res*. 2019;115(7):1244–1255. doi:10.1093/cvr/cvz066
41. Ding K, Chen L, He J, et al. Tetrahydropalmatine alleviates hyperlipidemia by regulating lipid peroxidation, endoplasmic reticulum stress, and inflammasome activation by inhibiting the TLR4-NF-kappaB pathway. *Evid Based Complement Alternat Med*. 2021;2021:6614985. doi:10.1155/2021/6614985
42. Sousa FM, Abd JA, Stannard GA, et al. Hypoxia-inducible factor 1 signalling, metabolism and its therapeutic potential in cardiovascular disease. *Biochim Biophys Acta Mol Basis Dis*. 2019;1865(4):831–843. doi:10.1016/j.bbadis.2018.09.024
43. Gao Q, Guan L, Hu S, et al. Study on the mechanism of HIF1a-SOX9 in glucose-induced cardiomyocyte hypertrophy. *Biomed Pharmacother*. 2015;74:57–62. doi:10.1016/j.biopha.2015.07.009
44. Huang X, He Z, Jiang X, et al. Folic acid represses hypoxia-induced inflammation in THP-1 cells through inhibition of the PI3K/Akt/HIF-1alpha pathway. *PLoS One*. 2016;11(3):e151553.